2014 13th International Conference on Control, Automation, Robotics & Vision
Marina Bay Sands, Singapore, 10-12th December 2014 (ICARCV 2014)

Blood Vessel Feature Description for Detection of Alzheimers Disease

Musab Sahrim and Mark S. Nixon
School of Electronic and Computer Science
University of Southampton
Southampton, United Kingdom
{ms14g11&msn}@ecs.soton.ac.uk

Roxana O. Carare
School of Medicine
University of Southampton
Southampton, United Kingdom
R.O.Carare@soton.ac.uk

Abstract— **We describe how image analysis can be used to detect the presence of Alzheimer's disease. The data are images of brain tissue collected from subjects with and without Alzheimer's disease. The analysis concentrates on the shape and structure of the blood vessels which are known to be affected by amyloid beta, whose drainage is affected by Alzheimer's disease.**
The structure is analysed by a new approach which measures the Influence of the blood vessels' branching structures. Their density and tortuosity are analysed in conjunction with a boundary description derived using Fourier descriptors. These measures form a feature vector which is derived from the images of brain tissue, and the discrimination capability shows that it is possible to detect the presence of Alzheimer's disease using these measures and in an automated way. These measures also show that shape information is influenced by the vessels' branching structure, as known to be consistent with Alzheimer's disease evolution.

***Keywords*— medical image analysis; Alzheimer's disease; segmentation; shape description.**

I. INTRODUCTION

Alzheimer's disease (AD) is the commonest form of dementia, affecting over 800,000 people in the UK and with no efficient treatment. Diagnosis is difficult, as many neurodegenerative conditions present with a similar picture [1]. Amyloid beta (Aβ) is a normal product of metabolism, cleaved from an amyloid precursor protein (APP) [2]. Young brains are equipped with different mechanisms to break down and eliminate Aβ, but with ageing and on the background of different genotypes the elimination of Aβ fails, leading to its accumulation and to AD[3]. The accumulation of Aβ in the walls of blood vessels of the brain reflects a failure of its elimination along the walls of blood vessels[4].

In recent years, researchers have tried to detect AD in the human brain using image processing techniques. Most of them have used MRI and CT scans to detect the abnormalities in the human brain including texture and shape abnormalities. For example, Li detected the shape changes of corpus callosum in AD [5]. In addition, Freeborough evaluated a texture feature vector to discriminate the AD with the normal brain [6], while Fischl introduced a new method to measure the thickness of the human cerebral cortex by considering the white and the grey matter[7]. However although the methods using computer vision have been demonstrated some detection capability, little attention has been given to detecting the abnormalities of specific components in the brain that are affected by amyloid beta, such as blood vessels. The concept of the early onset detection of AD has yet to receive much research attention. Naturally, any approach that can detect AD at the onset or early in its progression could be invaluable in medical planning.

Blood vessels have previously been analysed in diagnosis of diabetes, hypertension and atherosclerosis[8] supporting their potential use for diagnosing Alzheimer's disease. The importance of blood vessels towards diagnosing the disease has suggested the need for detection of the abnormalities of the blood vessels using computer vision. This is made difficult by the limited observations and understanding of blood vessels patterns. Natural pattern such as a sea fans[9], river deltas and trees show structural similarity that have yet to be understood by human and computer vision.

The detection of a blood vessel's pattern can use many features such as density and tortuosity which can be appropriate to define the blood vessels for Alzheimer's disease detection. To our knowledge, there has been no prior analysis of branching structure, especially in the analysis of blood vessels and in the diagnosis of Alzheimer's disease. In this study, we describe the branching structure of blood vessels by their density[10], by a new invariant measure of branching structure, and by their tortuosity. Our aim is to detect the signs of AD at early stage by focusing on the objects that have been most affected by this disease in early onset detection as the high density of blood vessels in Alzheimer's disease could show early sign of the disease and the inspiration of detection diabetes and other's disease by their tortuosity [8, 10]

A particular focus of this paper is the analysis of blood vessel shape for the detection of Alzheimer's disease. This confirms that the branching structure is consistent with the presence of Alzheimer's disease and confirms the influence of the branching structure on shape and on disease detection.

978-1-4799-5199-4/14/$31.00 ©2014 IEEE

II. Vessel Shape Description

We concentrate on blood vessel structure as there appears to be linkage between that and Alzheimer's disease. To achieve this, we first detect branching structure, and then analyse vessel shape.

Current approaches for analysing branching structures in medical images concentrate on ductal trees [7] and vascular structures [8]. These are mainly large scale analyses of topology whereas blood vessels in segments of brain tissue are considerably smaller. Further, there is no analysis of this sort directed towards the detection of Alzheimer's disease.

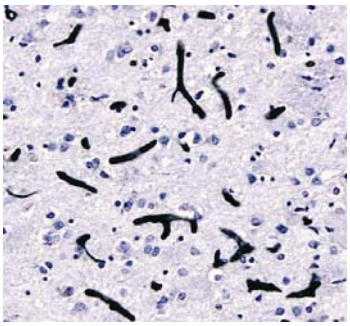

Figure 1: Example Image of Brain Tissue

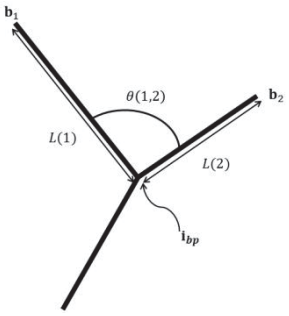

Figure 2: Branching Structure

A. Brain images

We used the slides with human tissue from the Brain Tissue Resource in Newcastle to acquire the images using a Nikon Eclipse E600 microscope fitted with a digital camera Nikon Coolpix 950 at ×10 magnifications. We have five samples of each tissue type, from: young, age-matched control and subjects with Alzheimer's disease. We choose images where the diagnosis was clear and the images are suitable for segmentation.

B. Density

Initially, we define the density as the number of branches in an image. In order to obtain the number of branches, we process the image to obtain a binary image and then convert it, via a thinning algorithm, into skeletons of vessels. Next, we seek to find the branching points so as to determine the intersections between them (should they occur) and thus count the number of branches.

The branching point $I(V)$, is calculated for each point V, of the structure (pixel) where the $N_i(V)$ are the neighbours of the analysed point, V, named clockwise consecutively. According to the equation below, $I(V)$ that has the value more than 2 will be classified as branching point I_{bp} as described in Eq 3(3).

$$I(V) = \frac{1}{2}\left(\sum_{i=1}^{8}\left|N_i(V) - N_{(i+1)mod8}(V)\right|\right) \quad (1)$$

$$\boldsymbol{i}_{bp} = I(V) > 2 \quad (2)$$

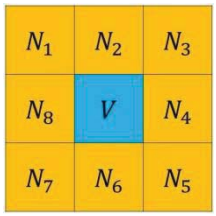

Figure 3: The template matching used to detect branching point of the images

After obtaining the branching points $\boldsymbol{i}_{bp} = (x_{bp}, y_{bp})$, the branching points are then excluded when counting the number of branches, $N_{branches}$ in the image. This was done by making the branching points, black, the same as the background image. The result obtained was the branches with no branching points, which were labelled to find the number of branches.

$$D = \sum\left(I_{vessel} \cap \overline{I_{bp}}\right) \quad (3)$$

C. Tortuosity

Tortuosity can be defined as the property of curve that has been twisted. As for the starting point, we use the basic measurement of tortuosity. This tortuosity measurement has been developed by Lotmar, Freiburghaus and Bracher[11] and tortuosity τ is describes as an arc-chord ratio

$$\tau = L/C \quad (4)$$

where L is a length of curve and C is the distance between the ends of curve. There is much room for extension in this measure and we investigate the basic form here as diagnostic and modelling of the vessel's branching structure.

D. Description of the Branching Structure

The detected branching points allow for a new analysis of the branching structure (Fig.2). Essentially we have segments of blood vessels which are at different inclinations to the branching points. For a branching point bp with N branches of length $L(bp)$ this can be described by the average vector product of pairs of branches and the angle between them, as in Eq. 5,

$$B = \sum_{i=1,N,j=1,N} L(i) \times L(j) \times \cos\left(\theta(i,j)\right) \Big/ N \quad i \neq j \quad (5)$$

As this equation appears to favour smaller angles, a version not using the cosine was also deployed, though this was found to have less capability for detecting the presence of Alzheimer's disease.

E. Boundary description using Fourier descriptor

Fourier descriptors (FD) have been shown to be an efficient way to recognise different shapes due to robustness to changes in scale, rotation, shifting and starting point. Furthermore, although the FD technique is already more than 40 years old, it has features that are easy to compute and robust to noise. To apply the Fourier descriptors, we need a perimeter contour. Fig.4 (b) shows the contour for an object with no branching points in Fig. 4(a). Fig.4(c) shows a vessel with one branching point and its contour in Fig. 4(d). The vessels will be analysed separately according to the number of branching points to investigate the relationship between branching and detection of Alzheimer's disease.

(a) vessel with no branching points | (b)contour from (a) | (c) vessel with one branching point | (d) contour from (c)

Figure 4. Vessels for Fourier Descriptor analysis.

Using Fourier descriptors, the high frequencies of the boundary will be ignored and the remaining low frequencies will be used to define the general shape properties of the object. Complex FDs are determined by applying the Fourier transform (FT) to find the frequency content of the whole shape by using the contour derived from shape boundary coordinates[12]. Based on frequency analysis, we can choose a small set of numbers, or, better known as the Fourier coefficient, which describes a shape rather than any noise. The curve in FD is described in two-dimensional (2D) whereas the image space is considered as complex plane. Thus, every pixel is represented by a complex number[12, 13].

$$s(k) = x(k) + jy(k) \tag{6}$$

The complex Fourier descriptors are derived by applying the Discrete Fourier Transform (the complex coefficients,$a(\mu)$)

$$a(\mu) = \sum_{k=0}^{K-1} s(k)\, e^{\frac{-j2\pi\mu k}{K}}, k = 0,1,2, \dots, K-1 \tag{7}$$

The inverse Discrete Fourier Transform for these coefficients restores $s(k)$

$$s(k) = \frac{1}{K}\sum_{\mu=0}^{K-1} a(\mu)\, e^{\frac{j2\pi\mu k}{K}}, k = 0,1,2, \dots, K-1 \tag{8}$$

We can create an approximate reconstruction of $\hat{s}(k)$if we use only the first P Fourier coefficients.

$$\hat{s}(k) = \frac{1}{P}\sum_{\mu=0}^{P-1} a(\mu)\, e^{\frac{j2\pi\mu k}{K}}, k = 0,1,2, \dots, K-1 \tag{9}$$

The FDs are normalized so as to be invariant to scaling, shifting, rotating and the starting point as in Table I.

TABLE I DETERMINING INVARIANT FDS

Transformation	Fourier Descriptor
Translation	$\tilde{a}(x) = a(x) + u_0\delta(x)$, where $\delta(x) = 1\ if\ k = 0$ and $\delta(x) = 0\ if\ k \neq 0$
Scaling or Zooming	$\tilde{a}(x) = \alpha a(x)$
Starting point	$\tilde{a}(x)e^{-i2\pi n_0/N}$
Rotation	$\tilde{a}(x) = a(x)e^{i\theta_0}, where\ e^{i\theta_0} = \cos\theta_0 + \sin\theta_0$

An alternative approach is to use Elliptic Fourier descriptors which are also have similar invariant with complex Fourier descriptors, but do not include the effects of high order frequencies that are more prone to noise [14].Let us denote $c'(t) = x'(t) + jy'(t)$ as the transformed contour. This contour is defined as,

$$\begin{bmatrix} x'(t) \\ y'(t) \end{bmatrix} = \frac{1}{2}\begin{bmatrix} a'_{x0} \\ a'_{y0} \end{bmatrix} + \sum_{k=1}^{\infty} \begin{bmatrix} a'_{xk} & b'_{xk} \\ a'_{yk} & b'_{yk} \end{bmatrix} \begin{bmatrix} \cos(k\omega t) \\ \sin(k\omega t) \end{bmatrix} \tag{10}$$

The advantage of these descriptors a' and b' with respect to complex FDs is that they do not involve negative frequencies. In Eq.11, the Elliptic Fourier Descriptor is also made invariant to contain neither the scale factor, nor rotation.

$$\frac{|A'_k|}{|A'_1|} = \frac{\sqrt{a_{xk}^2 + a_{yk}^2}}{\sqrt{a_{x1}^2 + a_{y1}^2}} \text{ and } \frac{|B'_k|}{|B'_1|} = \frac{\sqrt{b_{xk}^2 + b_{yk}^2}}{\sqrt{b_{x1}^2 + b_{y1}^2}} \tag{11}$$

For these descriptions, the vessels are labelled according to their branching level (Fig. 4) and the complex and the Elliptic FDs are calculated for $P = 64$ via Eqs. 7 and 11 respectively, for each image (separately for non-branching and branching vessels) and the mean of each FD for each vessel is obtained. This forms a feature vector of 64 components for each of the branching levels. The FDs for each image are then compared using *k*-NN classification to differentiate between AD and the normal images.

F. Classification

The features are then used for classification of AD. Features are assigned as vectors in the classification and *k*-NN classification is used since its implementation is fast and it suitable for small number of dataset. Clearly there are more sophisticated analyses possible, and faster ones, but here our intention is to investigate whether there is any promise in the use of these features and as such a basic classifier suffices.

Since we have a limited number of images, leave-one-out cross validation was deployed and merged with *k*-NN classification to determine the classification rate. We increased the value of *k* until 11 to determine the best value of k that in *k*-NN classification.

III. Result and Discussion

The first task was to determine which of the Fourier descriptors was most appropriate here. Fig. 5 shows the correct classification rates for the detection of Alzheimer's disease where the horizontal axis is the value of *k* used within the *k*-NN rule. Subjects with AD and recognised as such, together with subjects without AD and recognised as such, are both considered to be correct classifications. A subject without AD but recognised as a subject with AD, and vice versa, is marked as an incorrect classification. The correct classification rate is shown for the Complex and the Elliptic Fourier Descriptors of vessels that have a single branching point and the comparison is between the three groups (AD, age-matched control and young). The correct classification rate is the proportion of subjects correctly classified as having Alzheimer's disease or not averaged across the three groups. As can been the Complex FDs offer greater discrimination capability, and the trend of performance of both descriptors is very similar.

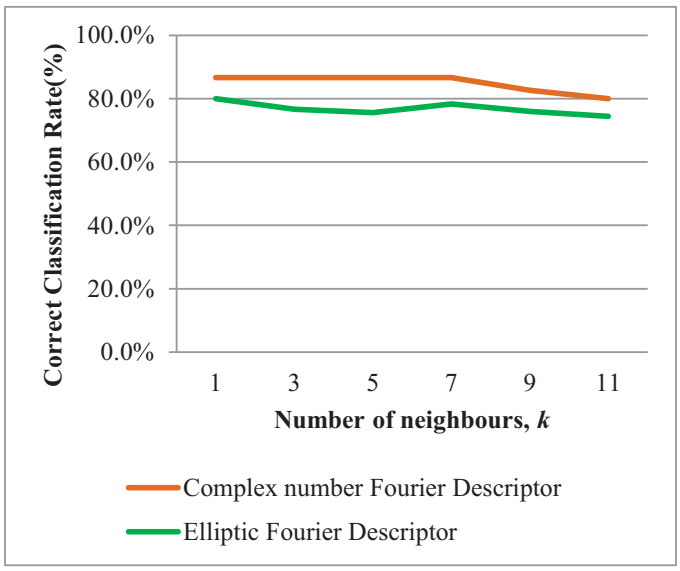

Figure 5. Correct classification rate for two different FD

We also investigated use of feature selection using Sequential Forward Floating Search (SFFS) [15] to find which coefficients contribute the most for correct classification. Table 2 lists the descriptors that offer the highest and the second-highest classification capability. It interesting that the results show the earlier coefficients are major contributors to correct classification, emphasizing the importance of overall shape. The distribution of the first and second most important descriptors is similar for the complex FDs and the EFDs, and the most important descriptions are different for vessels with branching structure, and vessels without branching structure, as expected.

Accordingly, Complex Fourier descriptors are chosen to perform the description as they show a better classification rate than Elliptic Fourier descriptors.

TABLE II: SELECTING THE MOST DISCRIMINATIVE FDS.

	Complex Fourier Descriptor		Elliptic Fourier Descriptor	
Comparison group	With Branching Point	Without Branching Point	With Branching Point	Without Branching Point
AD vs Young	(8) (14)	(3) (9)	(1) (13)	(12) (15)
AD vs age-matched control	(1) (7)	(3) (12)	(3) (7)	(5) (14)
Young vs old	(1) (7)	(2) (12)	(3) (7)	(5) (14)

To investigate the effect of branching structure we then separated the data into vessels with and without branching points for the three groups (AD, age-matched control and young). The correct classification rate is then the proportion of subjects correctly classified as having Alzheimer's disease or not averaged across the three groups. Clearly in this result (Fig. 6) the correct classification rate for the vessels with branching points show considerably higher performance than those without branching points. This suggests that the branching structure can be used to differentiate subjects with AD from those without AD as suspected by the effect of Alzheimer's disease on the drainage of Amyloid beta.

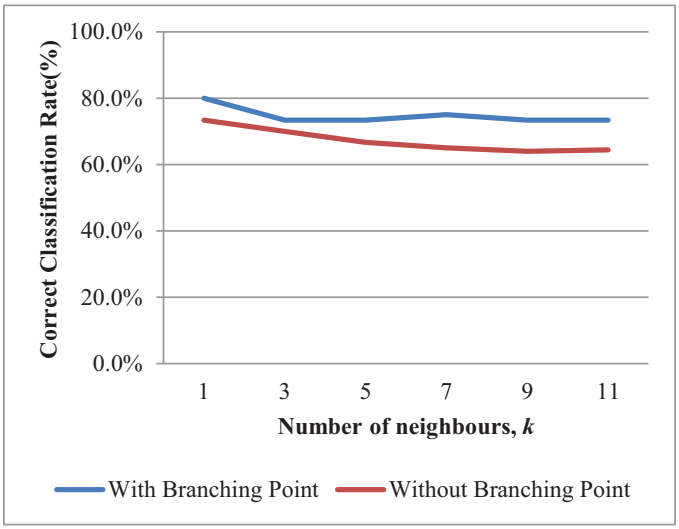

Figure 6. Correct classification rate for Complex FD for 3 groups (young, age-matched control and AD)

We then combined the vessels of young and age-matched control subjects as a single class of normal subjects and compared this with the vessels from subjects with AD to clarify the result (Fig. 7). Again this shows that branching structure aids recognition capability. The increase in recognition suggests that there is similarity in structure between the vessels of young and age-matched control subjects, further confirming the capability to use vessel shape description for the detection of AD.

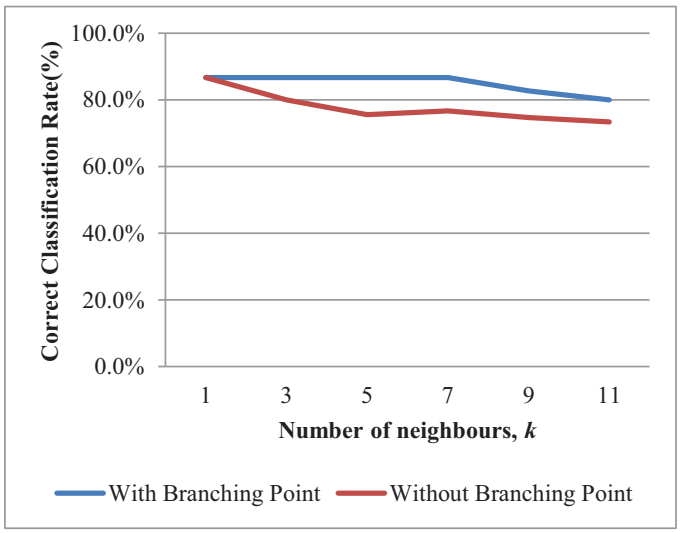

Figure 7. Correct classification rate for Complex FD for two groups (Normal and AD)

Figure 8 shows the Correct Classification Rate for the images when divided into three groups; young, old-matched control and old with Alzheimer's disease. The features used are the density D, the tortuosity, the branching measure B, and then FDs or combinations of these sets of measurements, combined as a feature vector for use with the *k*-NN rule. By this analysis, each measure contributes to successful discrimination of subjects with Alzheimer's disease, suggesting that image based analysis of brain tissue samples could prove a suitable avenue for research, as predicted by physical analysis and the postulated effects of Aβ. FDs are the most discriminative measures, followed by those relating to the branching structures. The tortuosity appears to offer the least sensitivity, but this might be due to the simplicity of the measure used, since the higher order FDs offer discriminative capability. The performance across differing values of *k* suggests that the feature space is quite smooth, since the recognition capability drops little with increase in *k*.

Next, in Fig. 6 we combine the young datasets with the control dataset to perform the discrimination of the brain tissue with AD from normal brain tissue. This provides ten images from young and age-matched control subjects, together with five samples from subjects with Alzheimer's disease.

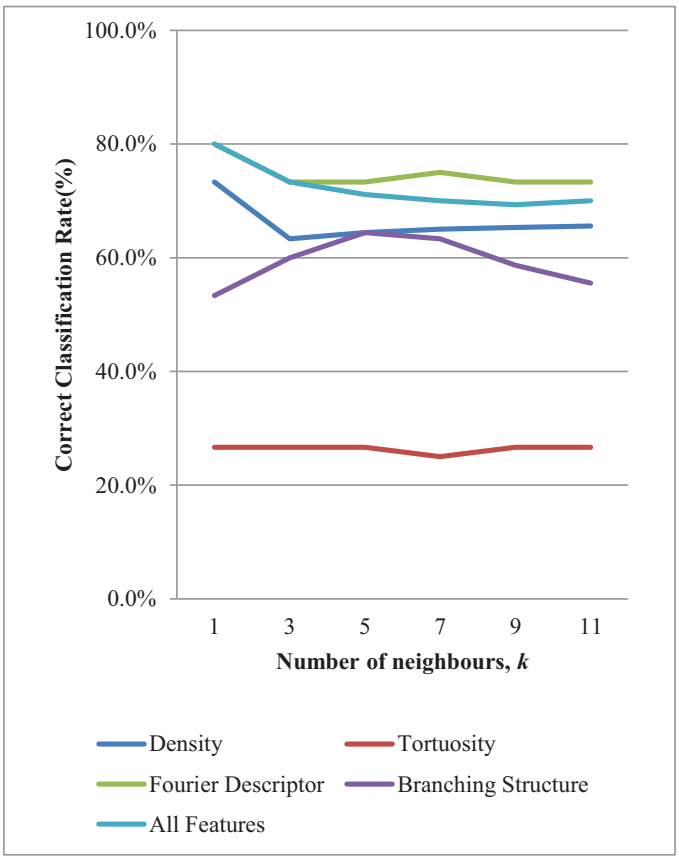

Figure 8. Correct classification rate and for each feature combinations versus the number of *k*.

Clearly in Fig. 9, the CCR for branching structure shows capability to differentiate the AD from other normal brain, but the feature space is less smooth. However, this measure of tortuosity shows increased performance, though the ranking of performance for the different measures remains the same. By combining all the features, we could see the classification rate are nearly 100% achievable suggesting all the features are important in this detection process. The performance analysis shows that it is possible to discriminate subjects with AD from those with AD. The analysis could potentially be improved with alternative methods for fusing the data, such as by classifier fusion, and by different measures (the tortuosity measure in particular is likely to be improved).

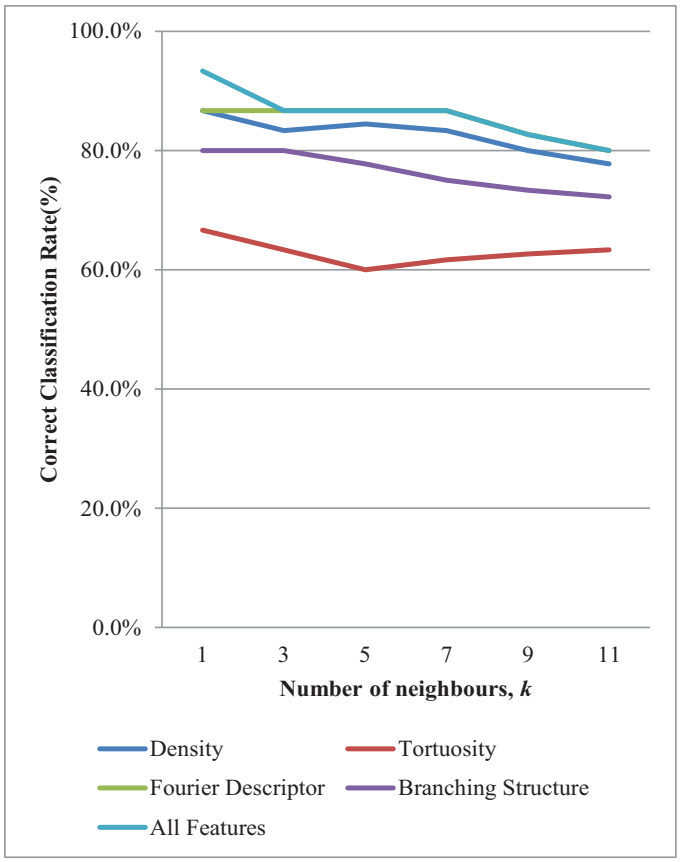

Figure 9. Correct classification rate overall and for each feature combinations versus the number of *k* using 2 groups.

IV. Conclusions

Studies suggest that the drainage of the protein Aβ is consistent with presence of Alzheimer's disease and this suggests that image based analysis of blood vessel structure might indicate the presence of Alzheimer's disease. Here we have deployed the standard measures of density and tortuosity for this analysis and have developed a new technique which is suited to analysis of the small branching structures to be found in these images. The images were derived from brain tissue of subjects in controlled conditions. We have performed the boundary analysis of vessels using Fourier Descriptors as the most discriminative feature in the recognition analysis. These two measures (branching structure and FDs) are formulated to have requisite invariant properties for this analysis.

We have shown that it is possible by these measures to discriminate between subjects with Alzheimer's disease and those without AD. In general, our initial result shows that the branching structure appears to be a major contributor to discriminate AD from a normal brain. This is reflected in the description by complex FDs, especially of the vessels with branching points. Branching structure is also discriminative as well as other features (density and tortuosity). The tortuosity has shown some contribution even though as per feature, it shows slightly lower performance compared with others and motivates the need for a better way to analyse tortuosity. The study so far has concentrated on features rather than classification and that and fusion could be more sophisticated though the approaches here suffice to demonstrate basic performance.

Note that so far the study is in vitro and this study is sufficiently encouraging for translation to in vivo 3D MRI image analysis.

References

[1] E. Boscolo, M. Folin, B. Nico, C. Grandi, D. Mangieri, V. Longo, *et al.*, "Beta amyloid angiogenic activity in vitro and in vivo," *International journal of molecular medicine,* vol. 19, p. 581, 2007.

[2] C. Lemere, J. Blusztajn, H. Yamaguchi, T. Wisniewski, T. Saido, and D. Selkoe, "Sequence of deposition of heterogeneous amyloid beta-peptides and APO E in Down syndrome: implications for initial events in amyloid plaque formation," *Neurobiology of disease,* vol. 3, p. 16, 1996.

[3] K. G. Mawuenyega, W. Sigurdson, V. Ovod, L. Munsell, T. Kasten, J. C. Morris, *et al.*, "Decreased clearance of CNS β-amyloid in Alzheimer's disease," *Science,* vol. 330, pp. 1774-1774, 2010.

[4] R. Weller, M. Subash, S. Preston, I. Mazanti, and R. Carare, "Perivascular Drainage of Amyloid-b Peptides from the Brain and Its Failure in Cerebral Amyloid Angiopathy and Alzheimer's Disease," *Brain Pathology,* vol. 18, pp. 253-266, 2008.

[5] L. Wang, F. Beg, T. Ratnanather, C. Ceritoglu, L. Younes, J. C. Morris, *et al.*, "Large deformation diffeomorphism and momentum based hippocampal shape discrimination in dementia of the Alzheimer type," *IEEE Trans Med Imaging,* vol. 26, pp. 462-70, Apr 2007.

[6] P. A. Freeborough and N. C. Fox, "MR image texture analysis applied to the diagnosis and tracking of Alzheimer's disease," *IEEE Trans Med Imaging,* vol. 17, pp. 475-9, Jun 1998.

[7] B. Fischl and A. M. Dale, "Measuring the thickness of the human cerebral cortex from magnetic resonance images," *Proc Natl Acad Sci U S A,* vol. 97, pp. 11050-5, Sep 26 2000.

[8] G. Kojda and D. Harrison, "Interactions between NO and reactive oxygen species: pathophysiological importance in atherosclerosis, hypertension, diabetes and heart failure," *Cardiovascular research,* vol. 43, pp. 652-671, 1999.

[9] L. Droz and G. Bellaiche, "Rhone deep-sea fan: morphostructure and growth pattern," *Am. Assoc. Pet. Geol., Bull.;(United States),* vol. 69, 1985.

[10] K. E. Biron, D. L. Dickstein, R. Gopaul, and W. A. Jefferies, "Amyloid triggers extensive cerebral angiogenesis causing blood brain barrier permeability and hypervascularity in Alzheimer's disease," *PLoS One,* vol. 6, p. e23789, 2011.

[11] W. Lotmar, A. Freiburghaus, and D. Bracher, "Measurement of vessel tortuosity on fundus photographs," *Graefe's Archive for Clinical and Experimental Ophthalmology,* vol. 211, pp. 49-57, 1979.

[12] M. Nixon and A. S. Aguado, *Feature Extraction & Image Processing for Computer Vision*: Academic Press, 2012.

[13] G. H. Granlund, "Fourier preprocessing for hand print character recognition," *Computers, IEEE Transactions on,* vol. 100, pp. 195-201, 1972.

[14] C. T. Zahn and R. Z. Roskies, "Fourier descriptors for plane closed curves," *Computers, IEEE Transactions on,* vol. 100, pp. 269-281, 1972.

[15] A. Jain and D. Zongker, "Feature selection: Evaluation, application, and small sample performance," *Pattern Analysis and Machine Intelligence, IEEE Transactions on,* vol. 19, pp. 153-158, 1997.